

Genetic Variation, Simplicity, and Evolutionary Constraints for Function-Valued Traits

Joel G. Kingsolver,^{1,*} Nancy Heckman,² Jonathan Zhang,^{2,†} Patrick A. Carter,³ Jennifer L. Knies,⁴ John R. Stinchcombe,⁵ and Karin Meyer⁶

1. Department of Biology, University of North Carolina, Chapel Hill, North Carolina 27599; 2. Department of Statistics, University of British Columbia, Vancouver, British Columbia; 3. School of Biological Sciences, Washington State University, Pullman, Washington 99164; 4. Department of Molecular Biology and Chemistry, Christopher Newport University, Newport News, Virginia 23606; 5. Department of Ecology and Evolutionary Biology, University of Toronto, Toronto, Ontario, Canada; 6. Animal Genetics and Breeding Unit, University of New England, Armidale, New South Wales 2351, Australia

Submitted June 17, 2014; Accepted January 13, 2015; Electronically published April 6, 2015

Online enhancements: appendixes. Dryad data: <http://dx.doi.org/10.5061/dryad.8v1f4>.

ABSTRACT: Understanding the patterns of genetic variation and constraint for continuous reaction norms, growth trajectories, and other function-valued traits is challenging. We describe and illustrate a recent analytical method, simple basis analysis (SBA), that uses the genetic variance-covariance (\mathbf{G}) matrix to identify “simple” directions of genetic variation and genetic constraints that have straightforward biological interpretations. We discuss the parallels between the eigenvectors (principal components) identified by principal components analysis (PCA) and the simple basis (SB) vectors identified by SBA. We apply these methods to estimated \mathbf{G} matrices obtained from 10 studies of thermal performance curves and growth curves. Our results suggest that variation in overall size across all ages represented most of the genetic variance in growth curves. In contrast, variation in overall performance across all temperatures represented less than one-third of the genetic variance in thermal performance curves in all cases, and genetic trade-offs between performance at higher versus lower temperatures were often important. The analyses also identify potential genetic constraints on patterns of early and later growth in growth curves. We suggest that SBA can be a useful complement or alternative to PCA for identifying biologically interpretable directions of genetic variation and constraint in function-valued traits.

Keywords: continuous reaction norms, function-valued traits, genetic variation, genetic constraints, growth trajectories, simplicity, thermal performance curves, trade-offs.

Introduction

Understanding the patterns of genetic variation and genetic constraints for complex phenotypes is a major challenge

for evolutionary biologists (Schluter 2000). For multivariate traits, this is done in a quantitative genetic context, in which genetic variation is represented as a genetic variance-covariance (\mathbf{G}) matrix (Lande and Arnold 1983). \mathbf{G} matrices are frequently quantified in terms of their component eigenvectors (principal components [PCs]) and eigenvalues (variances) to identify “directions” (combinations of individual traits) that differ in genetic variation. However, the biological interpretation of the PCs is often difficult and subjective (Blows 2007). Similarly, a function-valued (FV) trait—a trait that is a function of some independent continuous index, such as body mass as a function of age—can be represented in terms of a genetic variance-covariance (G) function (Kirkpatrick and Heckman 1989). The PCs of a G function are similarly difficult to interpret, particularly when the G function is estimated by nonparametric methods (Kingsolver et al. 2001). Parametric methods can be easier to interpret biologically but can have important statistical limitations: usually the appropriate parametric model is unknown, and these methods assume that all phenotypic and genetic variation—and constraints on that variation—can be represented by a single parametric function (Kirkpatrick and Heckman 1989; Kirkpatrick et al. 1990). An alternative is to develop methods that quantify variation in specific directions of biological interest for particular types of FV traits. For example, the template modes of variation (TMV) method was developed to evaluate specific hypotheses about variation in thermal performance curves (TPCs; Izem and Kingsolver 2005). This nonlinear approach is valuable for TPCs but cannot be directly applied to other types of traits, functions, or index variables. We lack a more general method that can identify biologically interpretable directions for FV traits and that quantifies the variation associated with these directions.

* Corresponding author; e-mail: jgking@bio.unc.edu.

† Present address: Department of Economics, Stanford University, Stanford, California 94305.

Am. Nat. 2015. Vol. 185, pp. E166–E181. © 2015 by The University of Chicago. 0003-0147/2015/18506-5558\$15.00. All rights reserved.
DOI: 10.1086/681083

In this study, we describe and illustrate a recent analytical method that can quantify variation in curves in terms of simplicity (Gaydos et al. 2013). The approach, here called simple basis analysis (SBA), quantifies variation in terms of simple, biologically interpretable directions based on quantitative metrics for the simplicity of a curve. The method was developed to visualize genetic constraints in curves; here, we emphasize its use for identifying and quantifying genetic variation in biologically informative directions. We have four main goals. First, we briefly review principal components analysis (PCA), showing how specific biological patterns of variation among curves generate PCs with specific shapes and how these shapes can reflect trade-offs. We do this by representing a curve as a vector and show how variation among curves can be quantified and visualized in terms of the eigenvectors (PCs) of the associated genetic variance-covariance matrix \mathbf{G} . Second, we use a case study of genetic variation in TPCs—clonal growth rates as a function of temperature—for bacteriophage to illustrate the direct parallels between PCA and SBA as alternative means to study genetic variability. SBA is defined in terms of a metric of simplicity and allows us to study genetic variability in both simple and more complex directions that can be easier to interpret than the directions arising in PCA. Third, we analyze simplicity for 10 estimated \mathbf{G} matrices from diverse organisms for two different types of FV traits: (1) TPCs for rates of population growth, mass increase, or locomotion as a function of temperature and (2) growth curves (GCs) of size as a function of age. Our goal is to determine the patterns of genetic variance in simple directions and whether these patterns differ between TPCs and GCs. Fourth, we review the idea of a “nearly null” subspace of \mathbf{G} —directions in which there is very little genetic variation—as a means of identifying genetic constraints on evolution. We use SBA to ask whether there are simple directions of genetic constraints in our data sets and whether these constraints differ between TPCs and GCs.

Methods and Results

Hypotheses about Variation in Curves

Let us first briefly review the strengths and limitations of PCA. PCA is a method for reducing the dimensionality of complex, multivariate data. It decomposes the variation represented by a variance-covariance matrix into a set of orthogonal PCs called eigenvectors. Any eigenvector defines a new variable equal to a linear combination of the original variables. The method proceeds by finding the vector of length 1, which represents a new variable that explains the greatest possible variance in the original var-

iables. The resulting vector is the first eigenvector of the variance-covariance matrix, and the new variable's variance is equal to the associated eigenvalue. The method then finds a second vector orthogonal to the first eigenvector that yields another new variable that explains the greatest amount of remaining variance, and so on. The full set of eigenvectors is a set of basis vectors that accounts for all of the variance in the original data, and the eigenvectors of the variance-covariance matrix are uncorrelated. Typically, most of the variation in the original data can be described by fewer eigenvectors than the number of original variables, which can be used as a smaller set of basis vectors, thus reducing the dimensionality of the problem. The loadings on each eigenvector describe the contribution of each of the original variables to the eigenvector. However, biological interpretation of the eigenvector loadings is often challenging and subjective.

We will use a simple example to illustrate different patterns of variation in biological curves and how they relate to the loadings on PCs associated with that variation. Consider a sample of genotypes from a bacteriophage population in which we measure TPCs for fitness (e.g., population growth rate as a function of temperature). The fitness of each genotype is measured at a fixed set of (e.g., nine) measurement temperatures. We are interested in visualizing and quantifying variation in TPCs among genotypes relative to the sample mean (fig. 1A, 1C, 1E). We consider three alternative and independent patterns of variation in TPCs. The first pattern, called vertical shift (fig. 1A), reflects variation in overall fitness across all temperatures: relative to the mean curve, a genotype with high fitness at one temperature has high fitness at all temperatures. A second pattern, called cooler-warmer (fig. 1C), describes a trade-off between fitness at lower and higher temperatures: in this case, individuals with relatively high fitness at low temperatures have relatively low fitness at high temperatures (and vice versa). A third pattern of variation involves a trade-off between thermal breadth and maximal fitness, called specialist-generalist (fig. 1E): here, individuals with higher maximal fitness at intermediate (optimal) temperatures have relatively low fitness at both low and high temperatures. These different hypotheses about variation have been widely explored by evolutionary physiologists interested in thermal adaptation (Huey and Kingsolver 1989; Angilletta 2009). In our hypothetical example, we envision these different patterns occurring in three different (imaginary) phage populations; in any real population, all three patterns may occur simultaneously (see below).

Suppose we consider the fitness of a genotype at each of the nine measurement temperatures to be a distinct but correlated trait. We can then view the TPC for each genotype as a multivariate vector of nine correlated traits

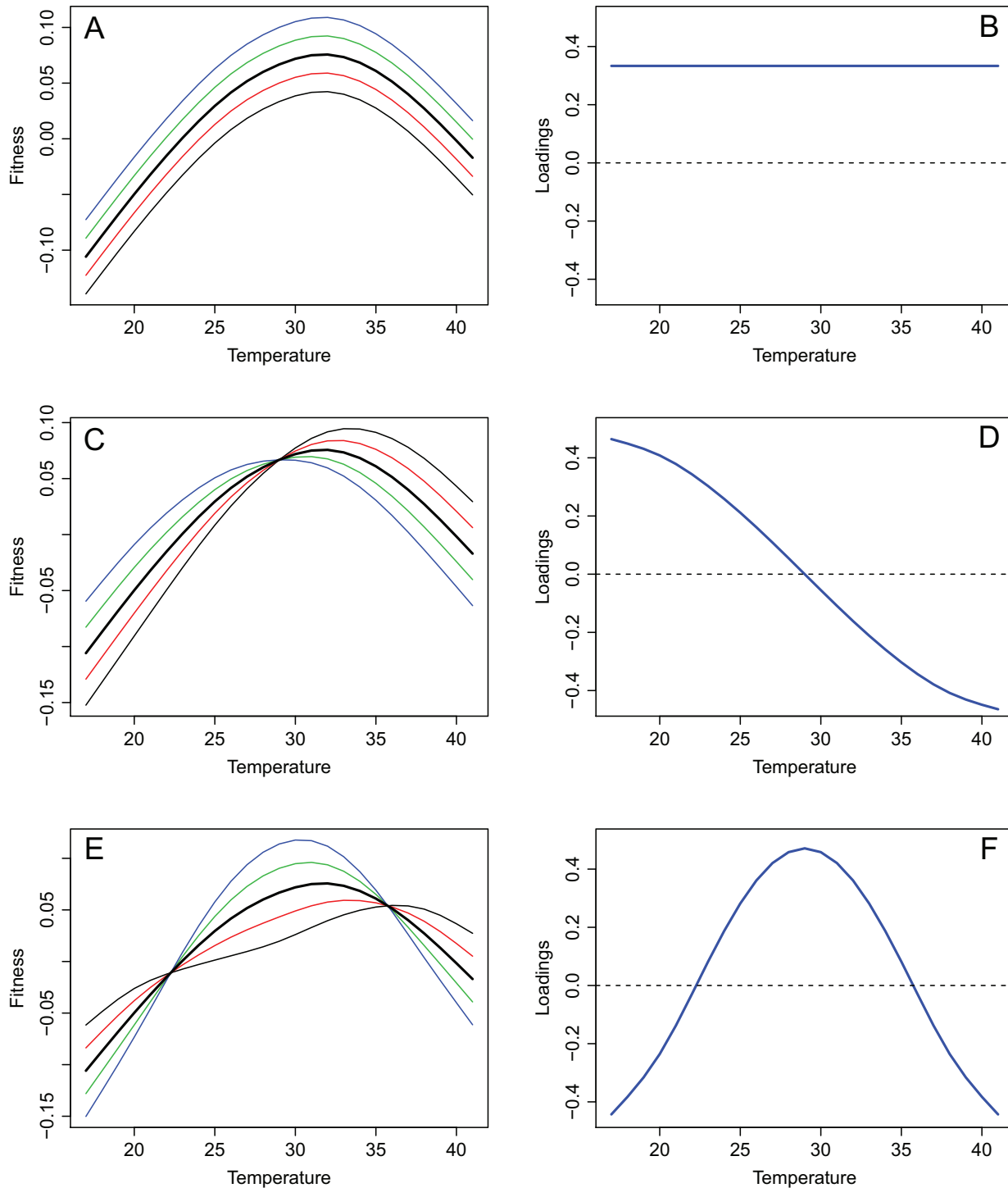


Figure 1: Examples of simple directions of genetic variation in thermal performance curves (TPCs) for fitness and the loadings on their associated principal components (PCs; eigenvectors), based on the G4 phage case study (see figs. 2, 3). *A, C, E*, TPCs (fitness as a function of temperature) for the mean curve (black) and for four clonal genotypes (other colors). *B, D, F*, PC loadings representing the variation in TPCs among genotypes. In these simple examples, a single PC (eigenvector) accounts for all of the variation in each case. *A, B*, Vertical shift variation. Loadings on the eigenvector are constant across all temperatures (a horizontal line), indicating overall variation in fitness among genotypes across all temperatures. *C, D*, Cooler-warmer variation. The eigenvector has positive loadings at cooler temperatures and negative loadings at warmer temperatures (or vice versa), indicating that genotypes with relatively high fitness at cooler temperatures have relatively low fitness at warmer temperatures (and vice versa). *E, F*, Generalist-specialist variation. The eigenvector has positive loadings at intermediate temperatures and negative loadings at both cold and hot temperatures (and vice versa), indicating that genotypes with relatively high fitness at intermediate temperatures have relatively low fitness at extreme cold or hot temperatures (and vice versa). See the main text for further description.

(Via and Lande 1985) and estimate the genetic variance-covariance matrix \mathbf{G} for this multivariate set of traits. A standard way of understanding variation in multivariate traits is via PCA of \mathbf{G} . In our simple example, each of the three different patterns of variation can be fully described by a single eigenvector that explains 100% of the genetic variation represented by \mathbf{G} (Kingsolver et al. 2001, 2015a). Now suppose that we plot the loadings of each eigenvector at each of the different measurement temperatures (fig. 1B, 1D, 1F). For the vertical shift example (fig. 1B), the loadings are identical (and nonzero) across all temperatures: genotypes have relatively high (or low) fitness at all temperatures. (Recall that a PC with all positive loadings is equivalent to one with all negative loadings—it is the change in sign across temperatures that is relevant.) For cooler-warmer (fig. 1D), the PC loadings are positive at cooler temperatures and negative at warmer temperatures (or vice versa), which indicates a reversal of relative fitness at low and high temperatures. In this sense, there are cool- and warm-adapted genotypes. Note that this pattern is related to but distinct from shifts in the position of the curve along the temperature axis, termed horizontal shift (Huey and Kingsolver 1989; Izem and Kingsolver 2005); horizontal shift involves a nonlinear deformation that cannot be fully represented by a single PC or other vector (Izem and Kingsolver 2005). For the specialist-generalist case (fig. 1F), the combination of positive loadings at intermediate temperatures with negative loadings at both low and high temperatures (or vice versa) indicates that specialist genotypes with high relative fitness at intermediate temperatures have low fitness at both low and high temperatures.

There are three key points from this simple example. First, there is a direct correspondence between the pattern of variation in curves and the loadings of the associated PCs. Different patterns of variation can generate different loadings with characteristic shapes (fig. 1). As a result, we can view a PC as a direction of genetic variation. Second, a plot of the PC loadings as a function of the index values (in this case, temperatures) allows us to visualize directions of variation among the curves. The loadings also provide a natural way to identify trade-offs: a trade-off involves changes in the relative rankings of fitness across temperature and is reflected in a change in the sign of the PC loadings across temperatures (fig. 1C–1F). Third, we constructed this simple example so that the three PCs represent interpretable, orthogonal directions of variation in the curves (fig. 1). Of course, in general this will not be the case for the eigenvectors of a variance-covariance matrix. As we illustrate in the next section, eigenvectors typically do not have such simple loadings or biological interpretations; we will use this to suggest an alternative approach to describing variation in curves based on the “simplicity” of the basis vectors.

Case Study: TPCs of G4 Phage

Data from real organisms rarely show the simple patterns of variation described in figure 1. In this section, we use data on TPCs for fitness of G4 phage to illustrate PCA and SBA as alternative and complementary approaches to characterizing genetic variation.

Knies et al. (2009) measured TPCs for population growth rate (fitness) at nine temperatures between 17° and 41°C for 15 genotypes of G4 phage sampled from field populations (fig. 2). These data were used to estimate the genetic (among-genotype) variance-covariance matrix \mathbf{G} . A standard PCA of the \mathbf{G} matrix shows that 98% of the total variance is described by the first seven PCs (eigenvectors). The loadings on the first six PCs (eigenvectors) are shown in figure 3. The first PC (fig. 3A), explaining 73% of the total variation, has small loadings at lower temperatures and larger positive loadings at higher temperatures (above 32°C). This suggests that there is smaller genetic variability in fitness at low temperatures but greater genetic variability in fitness at higher temperatures, a pattern that can be detected from the curves for each genotype (fig. 2). The other PCs are more complex in terms of the patterns of loadings on each eigenvector and are more difficult to interpret biologically.

We suggest that PCA alone may not be the most useful set of orthogonal basis vectors for quantifying and interpreting variation in TPCs and other FV traits. SBA provides an alternative and complementary set of orthogonal basis vectors that are defined in terms of the simplicity of the basis vectors (Gaydos et al. 2013). Appendix A (apps. A–C are available online) gives a more detailed description of the similarities in and differences between SBA and PCA. The method proceeds by finding the “simplest” basis vector, as defined by some metric of the simplicity of the vector (see below). The method then finds a second basis vector, the simplest vector that is orthogonal to the first basis vector, and so on. Just as with PCs, each basis vector corresponds to a new variable that is a linear combination of the original variables. The basis vectors in SBA are determined by the number of dimensions (here, the number of temperatures at which the traits are measured), the spacing between index values, and the metric of simplicity. By applying SBA to a \mathbf{G} or \mathbf{P} matrix, we can quantify the variance associated with each SB vector to provide insight into the sources of variation in the data. Similar to PCA, we can compute the SB score for each SB vector for each genotype or individual; the SB scores provide a new set of traits. Unlike PC scores, however, the SB scores for different SB vectors may be correlated (see below), even though the SB vectors are orthogonal. This method has recently been implemented in the R library *prinsimp* (Cubranic et al. 2013; Zhang et al. 2014).

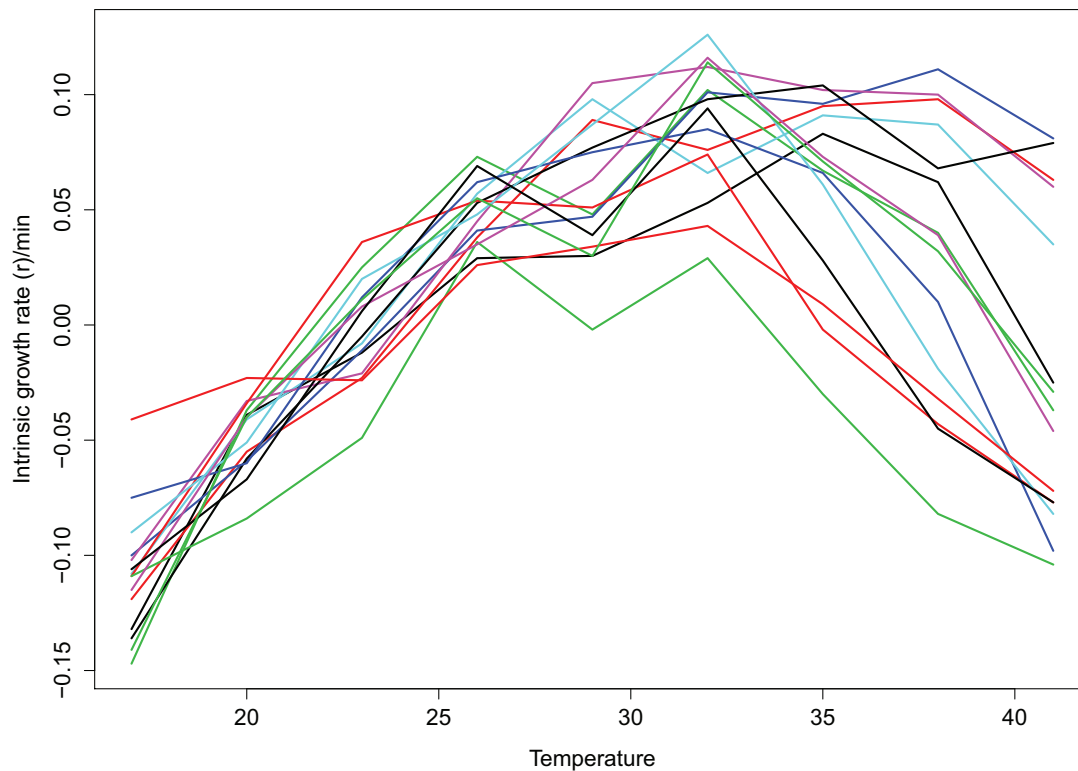


Figure 2: Population growth rate as a function of temperature for 15 genetic clones of G4 phage. Data are from Knies et al. (2009).

Figure 4 presents the SBA results for the G4 phage data, where the basis vectors are ordered from highest (SB1) to lowest in terms of simplicity. The first three SB vectors (SB1–SB3; see fig. 4) reflect the directions of variation described in our toy example above (fig. 1): vertical shift, cooler-warmer, and specialist-generalist. Vertical shift variation (SB1; fig. 4A) accounts for 32% of the total genetic variance, suggesting that there is substantial variance in fitness across all temperatures among these genotypes. Cooler-warmer variation (SB2; fig. 4B) accounts for the single greatest component of variance (40%), reflecting variation in adaptation to cooler or warmer temperatures. Specialist-generalist variation (SB3; fig. 4D) accounts for 11% of the variance, reflecting the trade-off between thermal breadth and maximal fitness at intermediate temperatures. These three simple directions of variation account for 83% of the total genetic variance of the TPCs. The remaining variance is accounted for by more complex basis vectors (e.g., SB4–SB6; fig. 4D–4F).

Thus far we have discussed “simple” in terms of biological patterns of variation (fig. 1), but we can define simplicity in more precise mathematical terms. Metrics of simplicity are used in statistical methods such as smoothing and penalized regression, where more complex (less

simple) functions are penalized in fitting models (Green and Silverman 1994). In developing SBA, Gaydos et al. (2013) considered quadratic metrics of simplicity based on first- and second-order differences, weighted by the distances between index values (to account for index values that are unevenly spaced). In this article, we use first-order differences; additional analyses with second-order differences (not shown) yielded qualitatively similar results. Zhang et al. (2014) provide a description of the method and its implementation in R (Zhang et al. 2014). Briefly, let \mathbf{v} be a vector that represents the evaluation of a function $f(\cdot)$ that is evaluated at K different values of t : $\mathbf{v} = \{v_1, v_2, \dots, v_k\}' = \{f(t_1), f(t_2), \dots, f(t_k)\}'$. Our simplicity metric is based on first divided differences:

$$D = \sum_j \frac{(v_j - v_{j-1})^2}{t_j - t_{j-1}}$$

The measure D is a good approximation of the integral of the square of the first derivative of the function f over all values of t : $D \approx \int (df/dt)^2$. Note that if f has a constant value for all values of t —that is, the graph of f is a horizontal line—then $D = 0$; nonzero values of the derivative of f will, in general, produce larger values of D . To create a measure that takes on larger values for simpler vectors

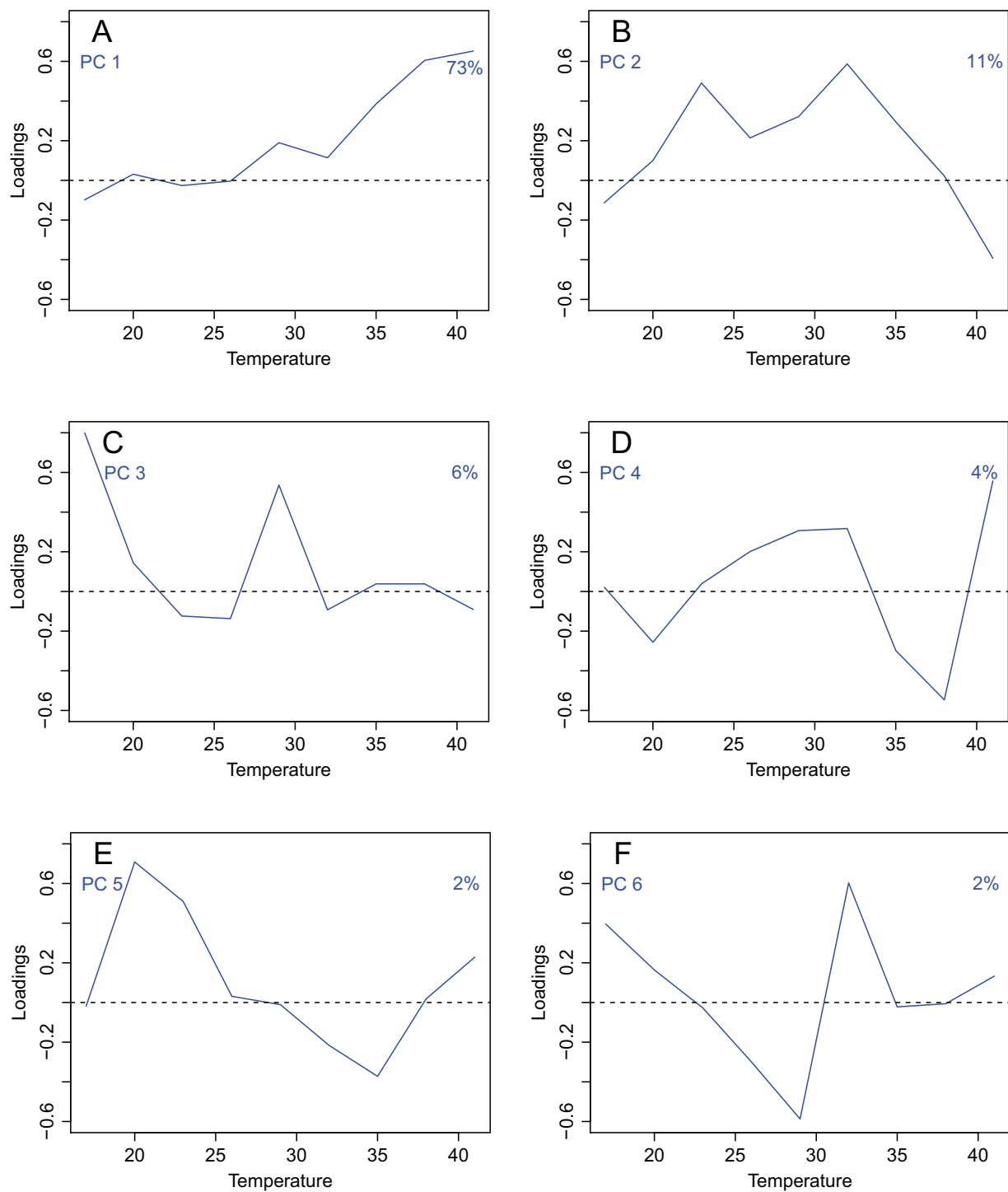


Figure 3: Principal component (PC) decomposition of genetic variation in thermal performance curves of population growth rate (fitness) for G4 phase. The loadings (as a function of temperature) for each of the first six eigenvectors (PC1–PC6) are shown (blue lines). The percentage of genetic variation explained by each PC is also indicated.

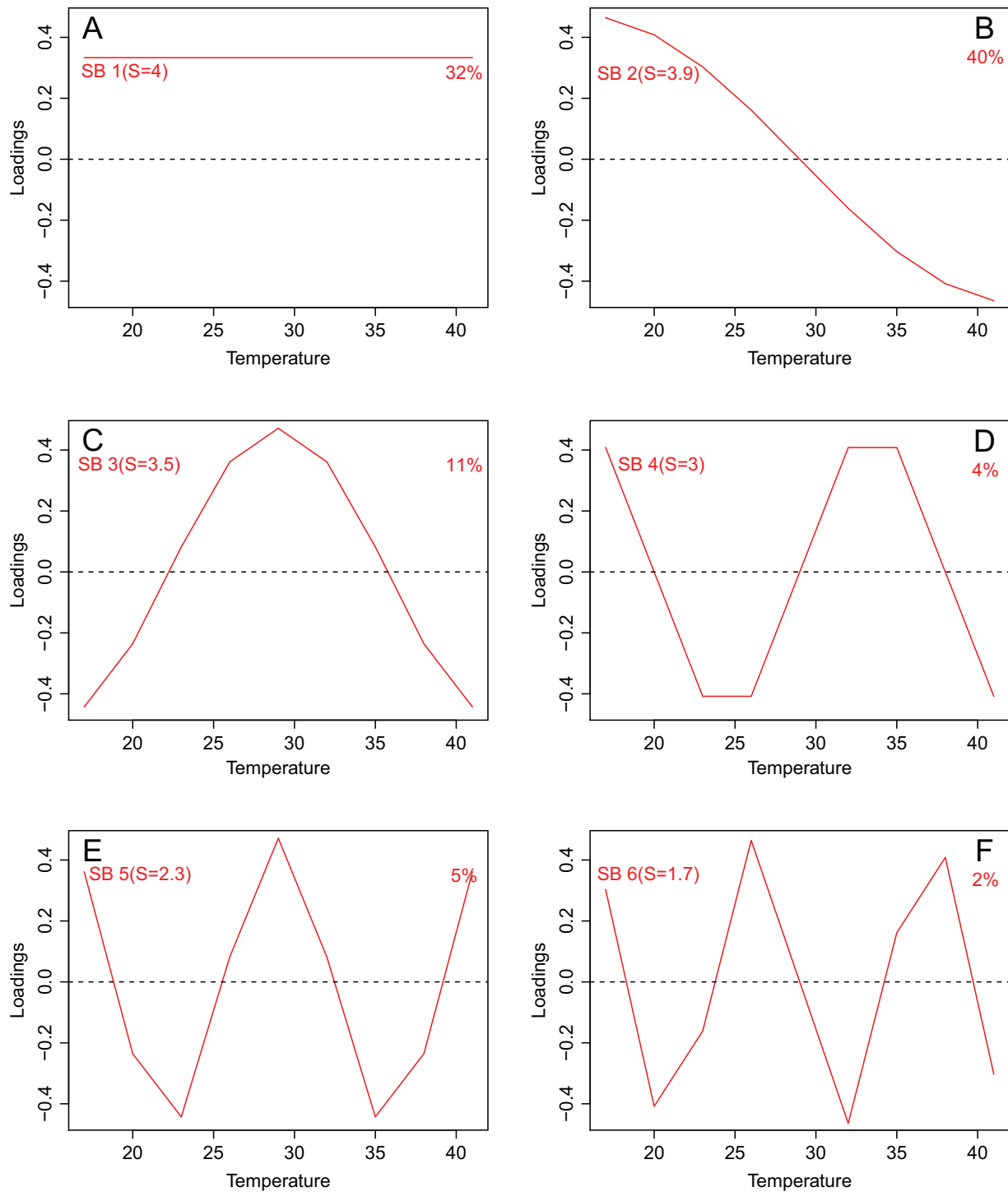


Figure 4: Simple basis (SB) decomposition of genetic variation in thermal performance curves of population growth rate (fitness) for G4 phage. The loadings (as a function of temperature) for each of the first six SB vectors (SB1–SB6) are shown (red lines). The percentage of genetic variation explained by each SB is also indicated.

\mathbf{v} , we define the simplicity metric S following Gaydos et al. (2013):

$$S = 4\mathbf{v}'\mathbf{v} - \min\{t_j - t_{j-1}\}D,$$

where \mathbf{v}' is the transpose of \mathbf{v} .

The simplicity metric S , based on first differences, takes on values ranging from a maximum simplicity of 4 (where the loadings for the SB vector are all equal, resulting in a horizontal line) to a minimum of 0 (where the loadings on the basis vector alternate between positive and negative values at different index values). Gaydos et al. (2013) provide a general method for defining simplicity measures based on other criteria for simplicity. In general, a vector's value of S is determined by the shape of the vector and the number and spacing of the index values (Zhang et al. 2014). In particular, the simplicity measure does not depend on the \mathbf{G} matrix. Therefore, the SB vectors are independent of the \mathbf{G} matrix, since these vectors are calculated using only the simplicity measure (see app. A). We order the SB vectors from highest to lowest simplicity (fig. 4). For our case study, the first three SB vectors (SB1–SB3) have S values of 4, 3.9, and 3.5, respectively. Note that as simplicity increases, the number of times the basis vector crosses 0—index values at which the loadings switch signs—decreases (fig. 4).

Figure 5 summarizes the results of the PCA and the SBA for the phage TPC data in terms of the simplicity and proportion of variance associated with each eigenvector (PCA) or SB vector (SBA). PCA orders eigenvectors in terms of the proportion of variance explained (right to left in fig. 4), regardless of simplicity; SBA orders basis vectors in terms of simplicity, regardless of the proportion of variance explained (top to bottom in fig. 5). For our purposes, the advantage of SBA is that it allows us to study the variance in simple, orthogonal directions that can be readily interpreted biologically (fig. 1). For the phage data, our analyses suggest that 40% of the genetic variation (SB2; fig. 4) is consistent with a cooler-warmer trade-off in which genotypes with relatively high fitness at higher temperatures have relatively low fitness at lower temperatures (fig. 1). Similarly, 32% of the variance (SB1; fig. 4) is associated with variation in overall fitness across all temperatures (vertical shift; fig. 1). More than 70% of the genotypic variation in TPCs for fitness can be accounted for in terms of two simple biological directions: vertical shift (SB1) and cooler-warmer (SB2; figs. 1, 4).

Our results emphasize that PCA and SBA are alternative and complementary methods for quantifying variation in biological curves. For the phage data, the first PC vector (73% of the total variation) indicates that there is greater genetic variation in fitness at higher rather than lower temperatures and that fitness at higher temperatures

is largely uncorrelated with fitness at low temperatures (figs. 2, 3). However, the other PCs are rather complex in shape and difficult to interpret in terms of genetic trade-offs. In contrast, SBA reveals that there is substantial genetic variation in two simple biological directions: vertical shift and cooler-warmer (fig. 1). This illustrates the advantages of SBA for interpreting patterns of variation. Conversely, PCA is more effective than SBA in reducing the dimensionality of the data: for example, a single PC (PC1) is associated with 73% of the total variation, whereas a single SB (SB2) is associated with 40% of the variation.

An important attribute of SBA is that, unlike PC scores, SB scores between different SB vectors can be correlated. For example, in the phage data set scores for SB1 are negatively correlated with those for both SB2 (−0.85) and SB3 (−0.39); because these scores are for genetic clones, these represent genetic correlations. This suggests that cooler-warmer (SB2) and specialist-generalist (SB3) trade-offs will reduce the rate of evolutionary response to selection on genetic variation in overall fitness across temperatures (SB1). In addition, scores for SB2 and SB3 are positively correlated (0.62), suggesting that genetic variation for these two types of trade-offs are not independent.

Patterns of Simplicity: Comparing TPCs and GCs

Our simplicity analyses with phage TPCs yielded two important results (figs. 4, 5). First, almost a third of the genetic variance in TPCs reflects overall variation in fitness across all temperatures (SB1). Second, more than half the genetic variance reflects genetic trade-offs across different temperatures, either between warmer versus cooler temperatures (SB2) or between specialists versus generalists (SB3). Do similar patterns occur in TPCs for other traits or study systems or in other kinds of FV traits? To explore this question, we consider thermal performances (TPCs) or GCs from a number of study systems. These two types of FV traits differ in several important ways. First, TPCs and GCs typically differ in shape: TPCs have a single maximal performance at some intermediate (optimal) temperature and decline to (or below) 0 at temperatures both below and above the optimum (figs. 1, 2). In contrast, most GCs start at a small initial size (at age 0) and then increase to a maximum, final size; in some cases, size declines below the maximum at older ages. In addition, changes in size with age (the slope and curvature of the GC) are constrained by the maximal achievable growth rates for an organism. For these reasons, patterns of genetic variation in GCs may be simpler and more constrained (see below) relative to those in TPCs of physiological or ecological rates.

We analyzed \mathbf{G} matrices or data for genetic clones obtained from published studies of TPCs (rate of fitness,

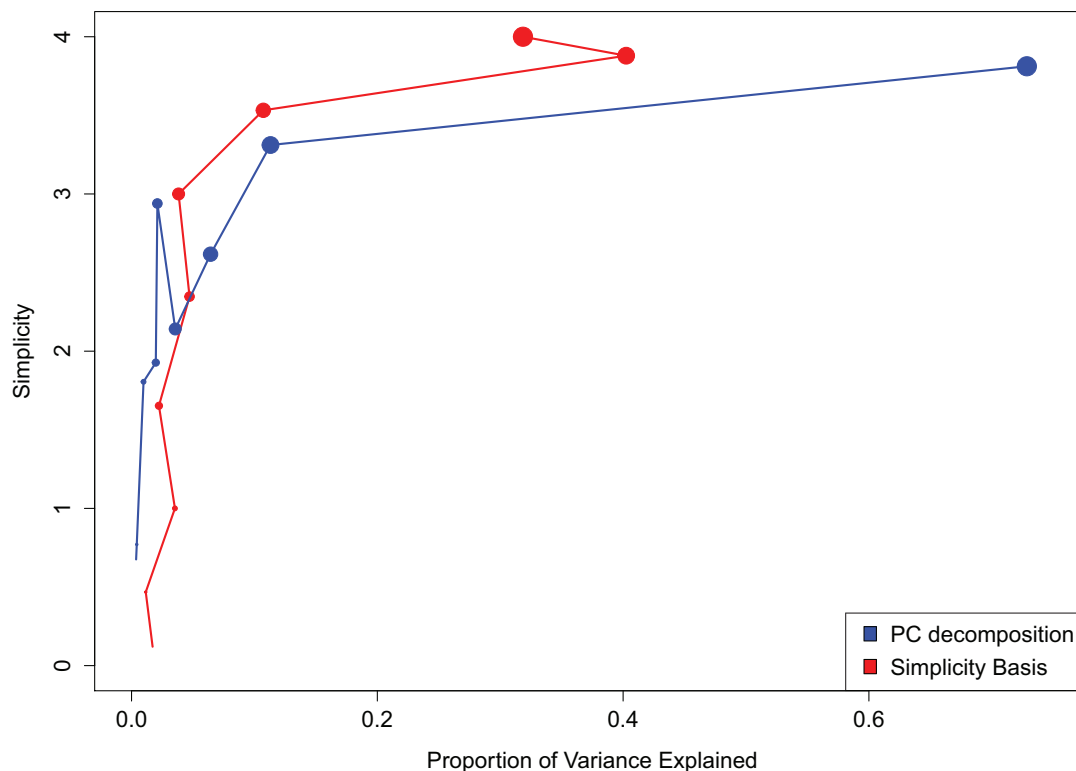


Figure 5: Simplicity (scaled from 0 to 4) as a function of the proportion of genetic variance explained for the basis vectors for thermal performance curves of population growth rate (fitness) for G4 phage. Results for both the principal component (PC) decomposition (blue points and lines) and the simple basis (SB) decomposition (red points and lines) are given. The order of the basis vector is indicated by the size of the point, from large (PC1 and SB1) to small (PC9 and SB9).

growth, or locomotion as a function of temperature) or GCs (size as a function of age). Each study measured performance or size at six or more (up to 13) index values and can provide either broad-sense or narrow-sense estimates of \mathbf{G} . We obtained five TPC and five GC data sets that included a range of organisms from viruses and bacteria to angiosperm and coniferous plants to insects and vertebrates (table 1; see app. C for further details about the data sets). This heterogeneous collection reflects the limited published data currently available that meet our criteria—the vast majority of relevant studies consider only one to three index values—but provide a useful starting point for exploring these issues. All \mathbf{G} matrices that were not previously published, along with sample R code for assessing the variability in estimates that depend on an estimated genetic covariance matrix, can be found in the Dryad Digital Repository: <http://doi.org/10.5061/dryad.8v1f4> (Kingsolver et al. 2015b).¹

1. Code that appears in *The American Naturalist* is provided as a convenience to the readers. It has not necessarily been tested as part of the peer review.

SBA of these data sets reveal several interesting patterns about simplicity and variation (fig. 6). First, recall that the first SB vector (SB1), with a simplicity score of $S = 4$ (largest points in fig. 6), reflects vertical shift variation. For the GC data sets (fig. 6B), SB1 is associated with 45%–72% of the genetic variance, suggesting that much of the variation in GCs reflects overall variation in size across all ages. In contrast, for the TPC data sets (fig. 6A) SB1 is associated with a much smaller fraction of the total genetic variance (12%–30%), suggesting that variation in overall performance across all temperatures is relatively limited. Second, SB2 (second largest points in fig. 6) is associated with 10%–40% of the genetic variance for both GCs and TPCs. This suggests that genetic trade-offs between size at early versus later ages and between performance at cooler versus warmer temperatures are common but do not explain the majority of variation in GCs and TPCs. Third, complex directions of variation (e.g., SB vectors with $S < 3$) are associated with a small fraction of the total genetic variance for the GCs (less than 10% of the total in all cases). In contrast, complex directions are often associated with a greater fraction of the total genetic variance for the TPCs, ranging from

Table 1: Partitioning of genetic variance into model (>98% of total genetic variance) and nearly null (<2% of total genetic variance) subspaces, for data sets from different organisms

Taxon	Type	Dimensions, no.		% null	Trait	Reference(s)
		Model	Nearly null			
<i>Pieris rapae</i>	TPC	4	2	33	Larval growth rate	Kingsolver et al. 2004
G4 phage	TPC	6	3	33	Population growth rate	Knies et al. 2009
<i>Escherichia coli</i>	TPC	8	3	27	Population growth rate	Bronikowski et al. 2001; Knies et al. 2009
<i>Salmonella</i>	TPC	7	4	36	Population growth rate	Bronikowski et al. 2001
<i>Aphidius ervi</i>	TPC	6	1	14	Walking speed	Gilchrist 1996
<i>Impatiens capensis</i>	GC	1	5	83	Plant height	Stinchcombe et al. 2010
<i>Ambystoma macrodactylum</i>	GC	3	3	50	Body length	Ragland and Carter 2004
<i>Pinus taeda</i>	GC	2	5	71	Plant height	Gwaze et al. 2002
<i>Mus domesticus</i>	GC	4	3	43	Body mass	Morgan et al. 2003
<i>Tribolium castaneum</i>	GC	4	2	33	Body mass	Irwin and Carter 2013

Note: The number of dimensions in the model and nearly null subspaces and the percentage of the total dimensions that are in the nearly null subspace (% null) are indicated for each species. GC = growth curve; TPC = thermal performance curve.

10% to more than 70% for particular SB vectors. These results suggest that patterns of genetic variance in GCs are simpler than those in TPCs (see “Discussion”).

Assessing variability in PCA and SBA of \mathbf{G} requires information about the sampling covariances among the elements of \mathbf{G} , not just the elements of \mathbf{G} and their associated standard errors. The underlying data for estimating \mathbf{G} are not available for many of our data sets, so we cannot assess variability in all cases. We use a subset of one of the data sets—GCs for *Tribolium castaneum* beetles (Irwin and Carter 2013)—to illustrate an approach to assessing variability (app. B). This is comprised of records at six selected ages, treated as individual traits in a multivariate analysis (rather than the FV approach taken by Irwin and Carter [2013]). Estimating sampling variation then, in brief, involves generating random samples from the estimated distribution of \mathbf{G} , calculating the functions of interest, and using their empirical distributions to determine their variability. Sampling error for the variance associated with each basis vector was generally similar for PC and SB vectors for this data set (fig. B1; figs. B1–B3 are available online). Estimated standard errors for the correlations between SB scores were relatively small for correlations between SB1, SB2, and SB3 but were larger for correlations involving SB5 and SB6 (table B1; tables B1, C1 are available online). The analyses also allow us to visualize variability in the loadings of the PCs (fig. B2). Sample R code for assessing the variability in estimates that depend on an estimated genetic covariance matrix can be found in the Dryad Digital Repository: <http://doi.org/10.5061/dryad.8v1f4> (Kingsolver et al. 2015b). The reader should keep in mind that an analysis without an assessment of sampling variability must be treated with caution.

Nearly Null Space and Genetic Constraints

We can use PCA and SBA in combination to detect genetic constraints and to describe them in biologically interpretable terms. Sometimes the genetic variation in a set of t traits or in a FV trait measured at t index values arises from a small number of traits—say from m ($<t$) combinations of the original traits (Lande 1979; Mezey and Houle 2005; Hansen and Houle 2008). When this occurs, the remaining $t - m$ “traits” can be viewed in a quantitative genetic framework as arising from genetic constraints and can be considered as phenotypic directions (combinations of traits) in which there is little or no genetic variation: phenotypic selection in these directions will lead to little or no evolutionary response (Lande 1979; Kirkpatrick and Lofsvold 1992). This set of phenotypic directions is simply the subspace spanned by the $n = t - m$ eigenvectors of the \mathbf{G} matrix with the smallest eigenvalues. This subspace contains little or no genetic variance; the subspace is called the null (no genetic variance) or nearly null (little genetic variance) subspace. Several authors have used PCA to quantify the dimensionality of genetic variance and of the null and nearly null subspaces (Mezey and Houle 2005). Both statistical and demographic criteria have been proposed to define the dimensionality of the nearly null subspace (Mezey and Houle 2005; Hansen and Houle 2008; Gomulkiewicz and Houle 2009; Gaydos et al. 2013).

Gaydos et al. (2013) proposed the use of SBA as a means of visualizing genetic constraints for FV traits—of finding simple phenotypic directions within the nearly null subspace. The analysis has two steps. First, PCA of the \mathbf{G} matrix is used to determine two subspaces: a model subspace (dimension m), which represents nearly all of the genetic

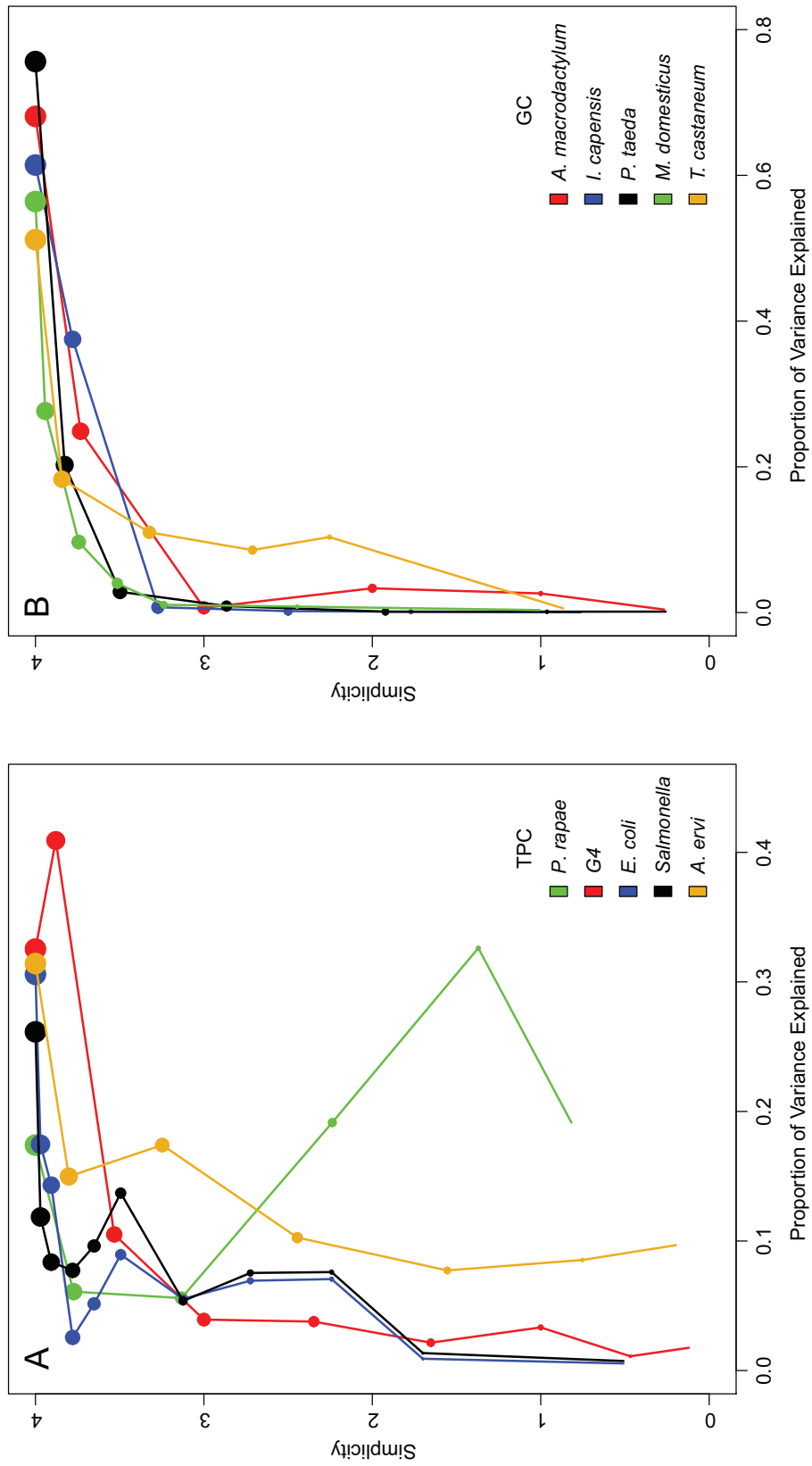


Figure 6: Simplicity (scaled from 0 to 4) as a function of the proportion of genetic variance explained for the simple basis (SB) vectors, for data sets from different organisms. The order of the basis vector is indicated by the size of the point. *A*, Thermal performance curves (TPCs) showing performance as a function of temperature. *B*, Growth curves (GCs) showing size as a function of age.

variance, and a nearly null subspace (dimension n), which has very little genetic variance. Second, SBA is used to identify the simplest directions (SB vectors) in the nearly null subspace on the basis of the simplicity metric S . The rationale is that these directions represent potential directions of phenotypic selection that are genetically constrained; these directions of selection may have straightforward biological interpretations (e.g., figs. 1, 4).

We apply this approach to our \mathbf{G} matrices for TPCs and GCs. In the absence of appropriate demographic information for these traits and study systems to define the nearly null space (Gomulkiewicz and Houle 2009), we choose the dimensionality of the model subspace (m) as representing at least 98% of the total genetic variance in \mathbf{G} ; the nearly null subspace (dimension $n = t - m$) then represents less than 2% of the genetic variance. (Analyses using a 99% cut-off give qualitatively similar results.) The results reveal an interesting contrast in the relative dimensionality of the model and nearly null subspaces for \mathbf{G} matrices of TPCs and GCs (table 1). The proportion of dimensions of \mathbf{G} in the nearly null subspace are consistently smaller for the TPC data sets (14%–36%) than for the GC data sets (33%–83%). This suggests that the structure of genetic variation is of lower dimension and more strongly constrained for GCs than for TPCs (see “Discussion”).

Directions in the nearly null subspace represent potential genetic constraints: directions in which phenotypic selection will lead to little or no evolutionary response. We can use simplicity analyses to identify and visualize the simplest direction (basis vector SB1) in the nearly null subspace for each \mathbf{G} matrix (fig. 7). For many of the TPC and GC data sets, the “simplest” direction in the nearly null subspace is quite complex, where the loadings change sign three or more times across the range of temperatures (TPCs) or ages (GCs). However, in some cases directions in the nearly null subspace are rather simple and readily interpretable as genetic constraints. For example, SB1 for the GC of *Impatiens capensis* (fig. 7B, blue line) has large positive loadings at early ages and negative loadings at late ages (and vice versa). This predicts that strong selection for relatively large size at early ages combined with selection for relatively smaller size at final ages would result in little evolutionary response. SB1 for the TPC of *Pieris rapae* (fig. 7A, green line) has similar loadings and a similar interpretation: strong selection for relative higher performance at low temperatures combined with selection for relative lower performance at high temperatures would result in little evolutionary response. In addition, SB1 for the GCs of *Tribolium castaneum*, *Ambystoma macrodactylum*, and *Pinus taeda* have positive loadings at both early and late ages and negative loadings at intermediate ages (fig. 7B). This suggests that selection for relatively large size at early and late ages combined with selection for relatively small

size at intermediate ages would result in little evolutionary response. These results illustrate how simplicity analyses of the nearly null subspace can help to identify and visualize potential genetic constraints on continuous reaction norms, GCs, and other FV traits.

Because the nearly null subspace is defined by using PCA, the dimension of the nearly null subspace is estimated with error, as are the loadings of SB vectors in the nearly null subspace. By randomly generating 10,000 \mathbf{G} matrices using the *T. castaneum* GC data set, we can assess this variability and also visualize variability in the loadings for the simplest SB vector in the nearly null subspace (app. B, fig. B3). The qualitative pattern of the loadings for the two-dimensional nearly null subspace (changing from negative to positive to negative with increasing age) is similar for most of the vectors, supporting the interpretation of a genetic constraint on GCs in this system.

Discussion

A major motivation for developing and implementing SBA is the difficulty of assigning biological interpretations of the PCs of \mathbf{P} and \mathbf{G} matrices for FV traits (Gaydos et al. 2013). PCs can in some cases have straightforward interpretations. For example, for sets of morphometric traits, the first PC is often associated with overall size (Schluter 2000). For GCs, the first PC often explains a large fraction of the total phenotypic and genetic variation and is often associated overall variation in size or growth across all ages (Kirkpatrick and Lofsvold 1992; Stinchcombe et al. 2010, 2012; Irwin and Carter 2013). Our analyses of GCs support this pattern: overall variation in size at all ages accounted for the majority of variation in each case (fig. 6). If the first PC dominates and its loadings are all of the same sign (i.e., the first PC is simple in shape), then PCA and SBA will give similar qualitative results and insights. In this case, PCA is preferable because PCs are by definition uncorrelated and PCA is more efficient in partitioning variation into its various components. Note that trade-offs across age, temperature, and other index variables imply that the PC or basis vector crosses 0 (fig. 1). In this sense, SBA may be more useful in identifying and interpreting genetic and phenotypic trade-offs (Kingsolver et al. 2015a).

A key rationale for the use of SBA is the notion that mathematically “simple” directions of phenotypic and genetic variation frequently have straightforward biological interpretations. We have provided several examples for performance curves—vertical shift, cooler-warmer, and generalist-specialist directions (figs. 1, 4)—where this is the case; Kingsolver et al. (2015a) provide analogous examples for GCs. These simple directions also have natural interpretations for patterns of phenotypic selection across

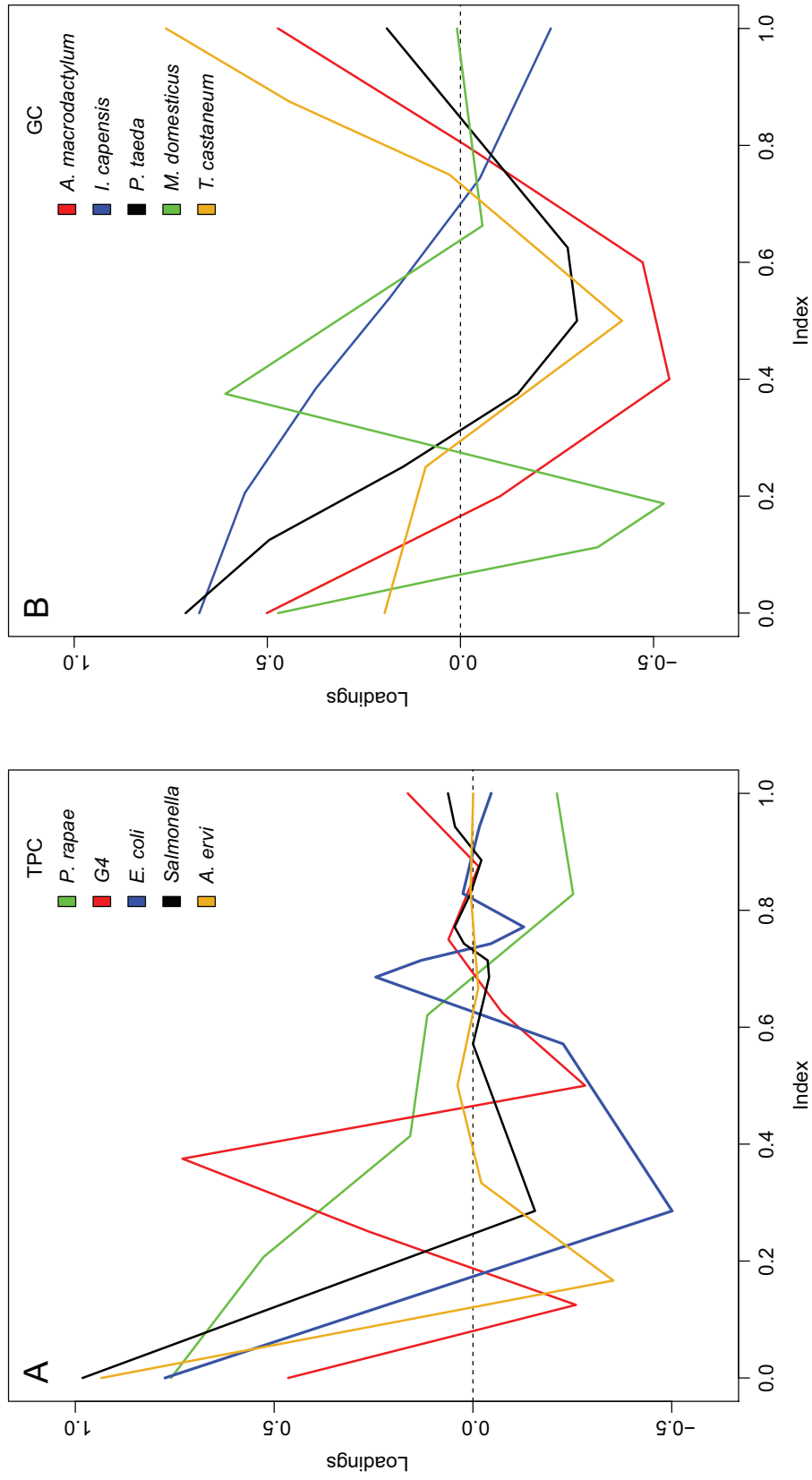


Figure 7: Loadings for the simplest basis vector (SB1) in the nearly null space of **G** for data sets from different organisms. These represent less than 1% of the total genetic variance in each case (see table 1). *A*, Thermal performance curves (TPCs) showing performance as a function of temperature. *B*, Growth curves (GCs) showing size as a function of age.

temperatures or ages. This is a primary motivation for SBA of the nearly null space of \mathbf{G} : to identify directions of phenotypic selection predicted to produce little or no evolutionary response. However, not all directions of biological interest are simple in the mathematical sense described here. For example, horizontal shifts in the position of performance curves or GCs represent nonlinear deformations that are not readily described by linear methods like PCA and SBA. Alternative approaches have been proposed and developed to quantify variation in horizontal shift and other nonlinear directions (Izem and Kingsolver 2005), but these are restricted to specific types of curves (e.g., performance curves).

In contrast to GCs, patterns of genetic variation in performance curves and continuous reaction norms are typically more complex and difficult to interpret, and the limitations of PCA have been widely noted in this context (Gilchrist 1996; Kingsolver et al. 2001, 2004; Knies et al. 2009). In our analyses of TPCs, overall variation in performance (fig. 1A, 1B) accounted for only 10%–30% of the genetic variation (fig. 6), and the loadings on the first PC changed sign in each case. For our case study with G4 phage, most of the PCs are quite difficult to interpret (fig. 3), whereas SBA suggests that substantial genetic variation is associated with three directions with straightforward biological interpretations (figs. 1, 4). The most valuable biological insight from this analysis is that 40% of the genetic variation is associated with a cooler-warmer trade-off in which genotypes with high performance at cooler temperatures have relatively low performance at warmer temperatures (fig. 1C, 1D). This cooler-warmer finding is consistent with previous analyses of these data using a semiparametric statistical method, TMV (Knies et al. 2006, 2009). TMV quantifies variation in TPCs in terms of parameters associated with vertical shift, optimal temperature, and thermal breadth (Izem and Kingsolver 2005). An important advantage of TMV is that it can directly account for nonlinear patterns of variation, including optimal temperature, which linear methods like PCA and SBA cannot. However, the TMV method is specific to performance curves and similarly shaped reaction norms, and it cannot be readily generalized to other curve shapes or trait types. SBA may be applied to data for any FV trait measured at multiple index values, regardless of curve shape (Gaydos et al. 2013). We note that curve shape—for example, whether curves are monotonic or unimodal—can alter the interpretation of the different SB vectors (for discussion, see Kingsolver et al. 2015a).

SBA can also provide useful insights into genetic constraints, through simplicity analyses of the nearly null space (Gaydos et al. 2013). Recent studies have explored the dimensionality of genetic variation and genetic constraints for multivariate and functional-valued traits, including wing shape in *Drosophila* (Mezey and Houle 2005) and GCs in

Tribolium beetles (Irwin and Carter 2013). Our analyses focus on a complementary issue: whether there are simple directions in the nearly null space representing patterns of phenotypic selection that would lead to little or no evolutionary response. Our results for GCs and TPCs identify several potential cases of such constraints (fig. 7). For example, the simplest basis vector in the nearly null space for *Ambystoma macrodactylum* indicates a lack of genetic variation for trade-offs between size at middle ages with size at early and late ages (fig. 7B). As a result, selection favoring small sizes (or low growth) at middle ages and larger sizes (or faster growth) at early and late ages would generate little evolutionary response (Gaydos et al. 2013; Kingsolver et al. 2015a). Interestingly, Ragland and Carter (2004) were able to detect this same result using PCA (Ragland and Carter 2004), supporting the notion that interpretation of patterns of genetic variation and constraint tend to be more straightforward for GCs than for TPCs. Similarly, the analyses indicate an analogous genetic constraint on cooler-warmer variation for TPCs of *Pieris rapae*, such that selection favoring slower relative growth rates at cooler temperatures and faster relative growth rates at warmer temperatures would generate little evolutionary response. Whether simple genetic constraints are more common for some types of organisms or traits remains an important evolutionary question.

An important challenge in evaluating patterns of genetic variation and constraint is the sampling error and statistical uncertainty in estimates of \mathbf{G} and its associated PCs and eigenvalues (Aguirre et al. 2014; Stinchcombe et al. 2014). We have illustrated one approach to assessing variability for PCA and SBA (app. B), by generating many estimates of \mathbf{G} using the inverse of the information matrix (sometimes referred to as the asymptotic covariance matrix of covariance parameters; app. B). The required information matrix is readily available from software like SAS, ASreml, and Wombat (Meyer and Houle 2013). An alternate approach is to sample \mathbf{G} s from the posterior distribution of \mathbf{G} by using Bayesian methods (Hadfield 2010; Morrissey et al. 2012; Aguirre et al. 2014; Stinchcombe et al. 2014). Note that using PCA or SBA on a covariance matrix does not require any distributional assumptions, but a multivariate normal assumption is needed to assess sampling variability in \mathbf{G} and in the variance associated with PCs and SBs (see app. B).

Berner (2012) has argued that, because of sampling error and the imprecision in estimating PCs, experimental studies will be more valuable than multivariate analyses for understanding genetic constraints on multivariate traits. However, recent selection experiments with *Drosophila* confirm that multivariate analyses of the nearly null subspace can identify important constraints on short-term evolutionary responses (Hine et al. 2014). Our analyses of vari-

ability for the simplest SB vector in the nearly null subspace (app. B, fig. B3) can identify qualitative patterns of genetic constraint. However, inferences about genetic constraint and the nearly null subspace will become increasingly problematic with decreasing sample sizes; for example, the G4 phage analyses are based on only 15 clonal genotypes.

Our analyses suggest interesting differences in patterns of genetic variation for GCs and TPCs. For our data sets, genetic variation in GCs was dominated by a single SB vector or PC explaining most of the total genetic variation, representing overall variation in size or growth rate across all ages; patterns of genetic variation in TPCs were more complex and heterogeneous. Several factors may contribute to this pattern. First, GCs are frequently monotonic increasing, whereas TPCs are unimodal and often asymmetric. Second, size is the cumulative outcome of growth and other processes over time, which may constrain the rate at which size may change with age. Conversely, physiological and locomotory rates may be more dynamic at shorter timescales. Third, more complex patterns of genetic variation involve trade-offs across environments (TPCs) or across ages (GCs). It is possible that trade-offs across environments are more common or important for performance curves and continuous reaction norms compared with life-history trade-offs across ages. Given that larger size is often selectively favored in many systems and ages (Kingsolver and Pfennig 2004), it is perhaps surprising that most of the standing genetic variance in GCs is in overall size, as we would expect consistent directional selection to reduce genetic variation in size. However, patterns of selection on size may also depend on environmental conditions: genotypes with larger sizes in one environment may be relatively smaller in other environmental conditions. In this case, heterogeneity in environmental conditions could generate variable selection and maintain genetic variation in size (Roff 2002). In addition, size and rates of growth and development can be genetically correlated with other fitness-related traits, including mortality (Mangel and Stamps 2001; Biro et al. 2004; Reinbold et al. 2009). Such genetic correlations can constrain the evolution of size and maintain substantial genetic variation in size within populations.

Acknowledgments

We thank G. Gilchrist for comments on the manuscript and S. Marron for discussion. J.G.K. was supported in part by National Science Foundation grant IOS-1120500. N.H. and J.R.S. were supported in part by the Natural Sciences and Engineering Research Council (NSERC) of Canada; J.Z. was supported in part by NSERC and by the Faculty of Science, University of British Columbia. J.G.K., N.H., J.R.S., K.M., and P.A.C. were supported in part by a grant

from the National Institute of Mathematical and Biological Synthesis to P.A.C.

Literature Cited

- Aguirre, J. D., E. Hine, K. McGuigan, and M. W. Blows. 2014. Comparing **G**: multivariate analysis of genetic variation in multiple populations. *Heredity* 112:21–29.
- Angilletta, M. J. 2009. *Thermal adaptation: a theoretical and empirical synthesis*. Oxford University Press, Oxford.
- Berner, D. 2012. How much can the orientation of **G**'s eigenvectors tell us about genetic constraints? *Ecology and Evolution* 2:1834–1842.
- Biro, P. A., M. V. Abrahams, J. R. Post, and E. A. Parkinson. 2004. Predators select against high growth rates and risk-taking behaviour in domestic trout populations. *Proceedings of the Royal Society B: Biological Sciences* 154:2233–2237.
- Blows, M. W. 2007. A tale of two matrices: multivariate approaches in evolutionary biology. *Journal of Evolutionary Biology* 20:1–8.
- Bronikowski, A. M., A. F. Bennett, and R. E. Lenski. 2001. Evolutionary adaptation to temperature. VII. Effects of temperature on growth rate in natural isolates of *Escherichia coli* and *Salmonella enterica* from different thermal environments. *Evolution* 55:33–40.
- Cubranic, D., J. Zhang, N. E. Heckman, T. L. Gaydos, and J. S. Marron. 2013. prinsimp: finding and plotting simple basis vectors for multivariate data. Comprehensive R Archive Network. Accessed November 2014. <http://CRAN.R-project.org/package=prinsimp>.
- Gaydos, T. L., N. E. Heckman, M. Kirkpatrick, J. R. Stinchcombe, J. Schmitt, J. G. Kingsolver, and J. S. Marron. 2013. Visualizing genetic constraints. *Annals of Applied Statistics* 7:860–882.
- Gilchrist, G. W. 1996. A quantitative genetic analysis of thermal sensitivity in the locomotor performance curve of *Aphidius ervi*. *Evolution* 50:1560–1572.
- Gomulkiewicz, R., and D. Houle. 2009. Demographic and genetic constraints on evolution. *American Naturalist* 174:E218–E229.
- Green, P. J., and B. W. Silverman. 1994. *Nonparametric regression and generalized linear models: a roughness penalty approach*. Chapman & Hall, London.
- Gwaze, D. P., F. E. Bridgwater, and C. G. Williams. 2002. Genetic analysis of growth curves for a wood perennial species, *Pinus taeda* L. *Theoretical and Applied Genetics* 105:526–531.
- Hadfield, J. 2010. MCMC methods for multi-response generalized linear mixed models: the MCMCglmm R package. *Journal of Statistical Software* 33:1–22.
- Hansen, T. F., and D. Houle. 2008. Measuring and comparing evolvability and constraint in multivariate characters. *Journal of Evolutionary Biology* 21:1201–1219.
- Hine, E., K. McGuigan, and M. W. Blows. 2014. Evolutionary constraints in high-dimensional trait sets. *American Naturalist* 184:119–131.
- Huey, R. B., and J. G. Kingsolver. 1989. Evolution of thermal sensitivity of ectotherm performance. *Trends in Ecology and Evolution* 4:131–135.
- Irwin, K. K., and P. A. Carter. 2013. Constraints on the evolution of function-valued traits: a study of growth in *Tribolium castaneum*. *Journal of Evolutionary Biology* 26:2633–2643.
- Izem, R., and J. G. Kingsolver. 2005. Variation in continuous reaction norms: quantifying directions of biological interest. *American Naturalist* 166:277–289.
- Kingsolver, J. G., S. E. Diamond, and R. Gomulkiewicz. 2015a. Curve thinking: understanding reaction norms and developmental tra-

- jectories as traits. Pages 39–54 in L. B. Martin, C. K. Ghalambor, and H. A. Woods, eds. *Integrative organismal biology*. Wiley Scientific, New York.
- Kingsolver, J. G., R. Gomulkiewicz, and P. A. Carter. 2001. Variation, selection and evolution of function-valued traits. *Genetica* 112:87–104.
- Kingsolver, J. G., N. Heckman, J. Zhang, P. A. Carter, J. L. Knies, J. R. Stinchcombe, and K. Meyer. 2015b. Data from: Genetic variation, simplicity, and evolutionary constraints for function-valued traits. *American Naturalist*, Dryad Digital Repository, <http://dx.doi.org/10.5061/dryad.8v1f4>.
- Kingsolver, J. G., and D. W. Pfennig. 2004. Individual-level selection as a cause of Cope's rule of phyletic size increase. *Evolution* 58:1608–1612.
- Kingsolver, J. G., G. J. Ragland, and J. G. Shlichta. 2004. Quantitative genetics of continuous reaction norms: thermal sensitivity of caterpillar growth rates. *Evolution* 58:1521–1529.
- Kirkpatrick, M., and N. Heckman. 1989. A quantitative genetic model for growth, shape, reaction norms, and other infinite-dimensional characters. *Journal of Mathematical Biology* 27:429–450.
- Kirkpatrick, M., and D. Lofsvold. 1992. Measuring selection and constraint in the evolution of growth. *Evolution* 46:954–971.
- Kirkpatrick, M., D. Lofsvold, and M. Bulmer. 1990. Analysis of the inheritance, selection and evolution of growth trajectories. *Genetics* 124:979–993.
- Knies, J. L., R. Izem, K. L. Supler, J. G. Kingsolver, and C. L. Burch. 2006. The genetic basis of thermal reaction norm evolution in lab and natural phage populations. *PLoS Biology* 4:1–8.
- Knies, J. L., J. G. Kingsolver, and C. L. Burch. 2009. Hotter is better and broader: thermal sensitivity of fitness in a population of bacteriophages. *American Naturalist* 173:419–430.
- Lande, R. 1979. Quantitative genetic analysis of multivariate evolution, applied to brain:body size allometry. *Evolution* 33:402–416.
- Lande, R., and S. J. Arnold. 1983. The measurement of selection on correlated characters. *Evolution* 37:1210–1226.
- Mangel, M., and J. Stamps. 2001. Trade-offs between growth and mortality and the maintenance of individual variation in growth. *Evolutionary Ecology Research* 3:583–593.
- Meyer, K., and D. Houle. 2013. Sampling based approximation of confidence intervals for functions of genetic covariance matrices. *Proceedings of the Association for the Advancement of Animal Breeding and Genetics* 20:523–526.
- Mezey, J. G., and D. Houle. 2005. The dimensionality of genetic variation for wing shape in *Drosophila melanogaster*. *Evolution* 59:1027–1038.
- Morgan, T. J., T. J. Garland, and P. A. Carter. 2003. Ontogenetic trajectories in mice selected for high wheel-running activity. I. Mean ontogenetic trajectories. *Evolution* 57:646–657.
- Morrissey, M. B., C. A. Walling, A. J. Wilson, J. M. Pemberton, T. H. Clutton-Brock, and L. E. B. Kruuk. 2012. Genetic analysis of life-history constraint and evolution in a wild ungulate population. *American Naturalist* 179:E97–E114.
- Ragland, G. J., and P. A. Carter. 2004. Genetic constraints on the evolution of growth and life history traits in the salamander *Ambystoma macrodactylum*. *Heredity* 92:569–578.
- Reinbold, D., G. H. Thorgaard, and P. A. Carter. 2009. Reduced swimming performance and increased growth in domesticated rainbow trout. *Canadian Journal of Fisheries and Aquatic Sciences* 66:1025–1032.
- Roff, D. A. 2002. *Life history evolution*. Sinauer, Sunderland, MA.
- Schluter, D. 2000. *The ecology of adaptive radiation*. Oxford University Press, Oxford.
- Stinchcombe, J. R., F.-V. T. W. Group, and M. Kirkpatrick. 2012. Genetics and evolution of function-valued traits: understanding environmentally responsive phenotypes. *Trends in Ecology and Evolution* 27:637–647.
- Stinchcombe, J. R., R. Izem, M. S. Herschel, B. V. McGoey, and J. Schmitt. 2010. Across-environment genetic correlations and the frequency of selective environments shape the evolutionary dynamics of growth rate in *Impatiens capensis*. *Evolution* 64:2887–2903.
- Stinchcombe, J. R., A. K. Simonsen, and M. W. Blows. 2014. Estimating uncertainty in multivariate responses to selection. *Evolution* 68:1188–1196.
- Via, S., and R. Lande. 1985. Genotype-environment interaction and the evolution of phenotypic plasticity. *Evolution* 39:505–522.
- Zhang, J., N. E. Heckman, D. Cubranic, J. G. Kingsolver, T. L. Gaydos, and J. S. Marron. 2014. Prinsimp. *R Journal* 6:27–42.

Associate Editor: Charles F. Baer
Editor: Troy Day